years for water on Venus, significantly reducing the need for continuous replenishment. The effect of a single large cometary impact (*22*) would also be proportionally diminished. Using different arguments, both Chyba (*24*) and Ip and Fernandez (*25*) concluded that Earth's oceans could have been provided by an early flux of comets—possibly tied to the formation of Uranus and Neptune. It is hard to see how this bombardment could have missed Venus. Unfortunately, the massive early escape of hydrogen required to remove an ocean of water would leave no record of D-H fractionation (*8, 20*); therefore, we cannot evaluate the size of the original reservoir from this ratio alone. Removal of an original, large water reservoir through dissociation and hydrogen escape (*4, 8*) appears to be the simplest explanation of the available data, however, provided such escape can occur in a way that does not affect the noble gases.

Our observations can easily be repeated at higher spectral resolution and for several locations on the planet at future inferior conjunctions of Venus. Additional data will improve the accuracy of the determination of the D/H ratio and the measurement of water abundance above 32-km altitude. If, as seems likely, radiation that has been detected from the dark side at shorter wavelengths (*26*) comes from still deeper levels in the atmosphere, it should ultimately be possible to reevaluate the global abundance of water vapor on Venus from Earth. This is now the greatest obstacle for efforts to understand the significance of the high value of the D/H ratio. Galileo observations of Venus made in February 1990 will also help. The prospect of Magellan radar maps with a resolution capable of detecting traces of ancient fluvial erosion adds yet another approach to the study of the history of water on Venus.

REFERENCES AND NOTES

1. J. S. Lewis, *Earth Planet. Sci. Lett.* **10**, 73 (1970).
2. J. C. G. Walker, K. K. Turekian, D. M. Hunten *J. Geophys. Res.* **75**, 3558 (1970).
3. K. K. Turekian and S. P. Clark, *J. Atmos. Sci.* **32**, 1257 (1975); E. Anders and T. Owen, *Science* **198**, 453 (1977). A third alternative, as discussed by W. M. Kaula [*ibid.* **247**, 1191 (1990)], is that much of the water on Venus is still trapped in the planet's interior. This hypothesis has not yet been developed in detail.
4. M. B. McElroy *et al.*, *Science* **215**, 1614 (1982).
5. H. A. Taylor, Jr. *et al.*, *J. Geophys. Res.* **85**, 7765 (1980).
6. H. Craig, *Science* **133**, 1833 (1961). This is the value measured in Standard Mean Ocean Water (SMOW).
7. R. E. Hartle and H. A. Taylor, *J. Geophys. Res. Lett.* **10**, 1965 (1983); S. Kumar and H. A. Taylor, Jr., *Icarus* **62**, 494 (1985). Kumar and Taylor reported values of the D/H ratio of 1.4×10^{-2} and 2.5×10^{-2} for two different orbits of the spacecraft.
8. T. M. Donahue *et al.*, *Science* **216**, 630 (1982).
9. J. L. Bertaux and J. T. Clarke, *Nature* **338**, 567 (1989).
10. T. Donahue, *ibid.* **340**, 513 (1989); J. L. Bertaux and J. T. Clarke, *ibid.*, p. 514. The ratio of intensities at Lyα (I_D/I_H) must be converted to the ratio of abundances (the D/H ratio) by means of a model for the hydrogen distribution in the upper atmosphere, which must in turn be consistent with the interpretation of the mass-2 ion as D^+ or H_2^+ (*4, 7*).
11. T. Owen *et al.*, *Science* **240**, 1767 (1988).
12. C. de Bergh *et al.*, *Bull. Am. Astron. Soc.* **21**, 926 (1989). This first attempt successfully recorded 15 Doppler-shifted lines of HDO in the ν_1 band at 3.7 μm. It was not possible however to record H_2O lines sufficiently nearby in the spectrum to avoid the large uncertainty inherent in radiative-transfer calculation of atmospheric opacity at widely varying wavelengths, and thus a useful value of the D/H ratio could not be obtained.
13. D. A. Allen and J. W. Crawford, *Nature* **307**, 222 (1984).
14. A 5-arc-second-diameter aperture was used, centered on a bright region located near 30° north latitude and 240° solar fixed longitude on the nightside of Venus. Individual spectra were co-added and apodized to provide a single spectrum with a resolution of $0.28\ \text{cm}^{-1}$ (FWHM) and a maximum signal-to-noise of about 50 (S/σ). Contamination by reflected sunlight from the bright side of Venus was removed by subtracting a scaled dayside spectrum recorded at a similar zenith angle. Absolute flux calibration was obtained from a spectrum of γ-Gem recorded during the same run.
15. B. Bézard *et al.*, *Nature* **345**, 508 (1990).
16. See D. Crisp [*Icarus* **67**, 484 (1986)] for a description of the treatment of scattering. The assumed thermal profile and cloud model are the same as in (*15*). In addition to molecular line absorption and cloud opacity, the atmospheric model incorporates a source of continuum absorption in the deep atmosphere that is needed to reproduce the depths of the CO_2 lines at wave numbers higher than $4350\ \text{cm}^{-1}$. The same value of the corresponding absorption coefficient estimated in (*15*), $\alpha = 7 \times 10^{-8}\ \text{cm}^{-1}\ \text{amagat}^{-2}$, is assumed throughout the entire window, including the 4120- to 4275-cm^{-1} region where the H_2O and HDO lines occur. This absorption alone limits the region of line formation to altitudes above 30 km (10 bars). A Lorentzian line shape was used for all absorbers except CO_2, which has a sub-Lorentzian line profile (*15*).
17. L. W. Esposito *et al.*, in *Venus*, D. M. Hunten, L. Colin, T. M. Donahue, V. I. Moroz, Eds. (Univ. of Arizona Press, Tucson, AZ, 1983), pp. 484–564.
18. U. von Zahn *et al.*, in *ibid.*, pp. 299–430.
19. The error bars for the CO mixing ratio are ±30%, taking into account the uncertainties on the atmospheric model. The derived mixing ratio is in relatively good agreement with the Pioneer Venus measurements, which yielded 30 ± 18 ppm at this altitude (*18*).
20. D. M. Hunten *et al.*, in *Origin and Evolution of Planetary and Satellite Atmospheres*, S. K. Atreya, J. B. Pollack, M. S. Matthews, Eds. (Univ. of Arizona Press, Tucson, AZ, 1989), pp. 386–422.
21. H. E. Revercomb *et al.*, *Icarus* **61**, 521 (1985).
22. D. H. Grinspoon, *Science* **238**, 1702 (1987); see also D. H. Grinspoon and J. S. Lewis, *Icarus* **74**, 21 (1988).
23. J. M. Rodriguez, M. J. Prather, M. B. McElroy, *Planet. Space Sci.* **32**, 1235 (1984).
24. C. F. Chyba, *Nature* **330**, 632 (1987); *ibid.* **343**, 129 (1990).
25. W. H. Ip and J. A. Fernandez, *Icarus* **74**, 47 (1988).
26. D. A. Allen, *Int. Astron. Un. Circ. 4962* (1990).

27. T.O. was supported in part by National Aeronautics and Space Administration (NASA) grant NGR 33015141 and National Science Foundation grant INT 8715243; B.L.L. was supported by NASA grant NAGW-1505; D.C. was supported in part by grants from the NASA Planetary Astronomy and Planetary Atmospheres Programs to the Jet Propulsion Laboratory, California Institute of Technology.

10 September 1990; accepted 12 December 1990

An Interplanetary Dust Particle Linked Directly to Type CM Meteorites and an Asteroidal Origin

J. P. BRADLEY AND D. E. BROWNLEE

Tochilinite, an ordered mixed-layer mineral containing Mg, Al, Fe, Ni, S, and O, has been identified in an interplanetary dust particle (IDP). This mineral is found in only one other class of meteoritic materials, type CM carbonaceous chondrites. The presence of tochilinite in an IDP provides a direct petrogenetic link between a member of the layer-silicate subset of IDPs and a specific class of meteorites and thus establishes that some IDPs collected in the stratosphere have an asteroidal origin. The scarcity of this IDP type suggests that materials with CM mineralogy are not abundant among the dust-producing asteroids.

EXTRATERRESTRIAL MATERIALS CAPtured by Earth include both conventional meteorites and micrometer-sized interplanetary dust particles (IDPs). Meteorites have been intensively studied because laboratory specimens have been available for many decades and most are large (>1 cm) objects that can be examined by multiple analytical techniques. The IDPs have been studied in less detail because most have been collected only during the past decade (*1*) and because techniques sensitive enough for analysis of nanogram quantities of material are required. Meteorites are believed to be derived primarily from asteroids (*2, 3*), but because only a few asteroids have spectral reflectances similar to those of the major meteorite classes (*4*), it appears that meteorites are a highly biased sampling. This bias is believed to result from two processes. First, for bodies larger than about $1\ \text{cm}^3$, only strong objects can survive atmospheric entry, and fragile objects, like cometary meteors and weaker asteroidal materials, fragment into dust (*5*). Second, the

---

J. P. Bradley, McCrone Associates, Westmont, IL 60559-1275.

D. E. Brownlee, Department of Astronomy, University of Washington, Seattle, WA 98195.

sources of conventional meteorites appear to be largely restricted to regions of the asteroid belt where orbital resonance with Jupiter initiates gravitational transfer to Earth-crossing orbits (*2*). Both comets and asteroids generate IDPs (*1, 6–8*), and IDPs include both strong objects as well as extremely fragile meteoritic materials that can survive atmospheric entry because of the greatly reduced ram pressure exerted on meteors less than about 1 mm^3 in size (*9*). Because the orbits of small particles decay to Earth-crossing under the influence of Poynting-Robertson drag (*1, 10, 11*), asteroidal IDPs can be derived from virtually any dust-producing region of the asteroid belt. One of the fundamental goals of interplanetary dust research is to identify IDPs that have an asteroidal origin, because they may provide a broader and less biased sampling of the asteroid belt than is provided by meteorites.

Among the collected IDPs are a group referred to as chondritic because their bulk elemental compositions generally agree with those of chondritic meteorites (*7*). One particular subset of chondritic IDPs are strong candidates for asteroidal materials because, like CI and CM meteorites, they contain abundant fine-grained layer silicates, carbonates, and related phases (*7, 12, 13*). The presence of these phases is indicative of an episode of aqueous alteration, which is believed to have occurred within moderately heated asteroids during the early history of the solar system (*14*). However, it has not been possible to link these "layer-silicate" IDPs directly to chondritic meteorites because no IDP has been found with a mineralogy characteristic of a specific class of meteorites. In this report, we describe a layer-silicate IDP that contains tochilinite, an ordered mixed-layer mineral containing Mg, Al, Fe, Ni, S, and O, that has been found within only one other class of meteoritic materials, the type CM carbonaceous chondrites. The finding of tochilinite establishes a direct petrogenetic link between an IDP and a class of meteorites, implies a common asteroidal provenance for this IDP, and focuses attention on the entire subset of layer-silicate IDPs as a diverse sampling of the hydrous asteroids.

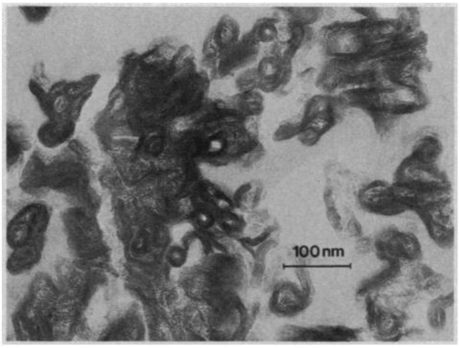

Fig. 2. Bright-field electron micrograph of a tochilinite-rich region of a thin section (~50 nm thick) of RB12A44. The concentric structures are tochilinite tubes (viewed in cross section). [See also Fig. 3D and compare with figures 13 and 14 of (*22*).] Many of the tochilinite tubes contain (noncrystalline) silicate cores.

Table 1. Compositions (normalized to that of Si) of matrix phases in RB12A44 and a type CM carbonaceous chondrite. (Column 1, bulk composition of the fragment of RB12A44 shown in Fig. 1A; column 2, average and standard deviations (parentheses) for ten individual thin sections of RB12A44; column 3, tochilinite-cronstedtite intergrowth in RB12A44; column 4, cronstedtite, $Mg_{0.61}Al_{0.39}Ca_{0.01}Fe^{2+}_{3.83}Fe^{3+}_{1.09}[Si_{2.63}Al_{0.39}Fe^{3+}_{0.98}]0_{10}(OH)_8$, in RB12A44; column 5, Mg-rich serpentine, $Mg_{3.94}Al_{0.21}Ca_{0.002}Mn_{0.02}Fe^{2+}_{1.65}[Si_{4.0}]0_{10}(OH)_8$, in RB12A44; column 6, tochilinite-cronstedtite intergrowth in Murray (CM) matrix (*22*); column 7, cronstedtite in Murray (CM) matrix (*22*); column 8, Mg-rich serpentine in Murray (CM) matrix (*22*).

Element	1	2	3	4	5	6	7	8
Mg	0.718	0.427 (0.089)	0.770	0.204	0.844	0.922	0.461	1.030
Al	0.113	0.195 (0.032)	0.361	0.281	0.049	0.332	0.118	0.036
S	0.503	0.348 (0.064)	2.980	0.012	0.003	3.052	0.197	0.172
Ca	0.033	0.010 (0.005)	0.016	0.006	0.008			0.003
Cr	0.023	0.023 (0.007)	0.065			0.015		
Mn	0.010	0.014 (0.004)	0.082	0.024	0.008			
Fe	2.433	2.677 (0.438)	10.672	4.462	0.814	10.759	4.261	0.801
Ni	0.100	0.074 (0.015)	0.442			0.339	0.016	0.053

The tochilinite and serpentine-bearing IDP, RB12A44, was collected from the stratosphere at an altitude of 18 to 20 km with the use of a NASA U-2 aircraft (*1*). It was found as a grouping of five 10- to 12-μm fragments of a larger (~30 μm) IDP that broke up when it impacted onto the collection substrate. We used the scanning electron microscope (SEM) to examine the bulk compositions, surface textures, and morphologies of the fragments and the analytical electron microscope (AEM) to investigate compositions and crystal structures of specific mineral phases (*15*). Particle

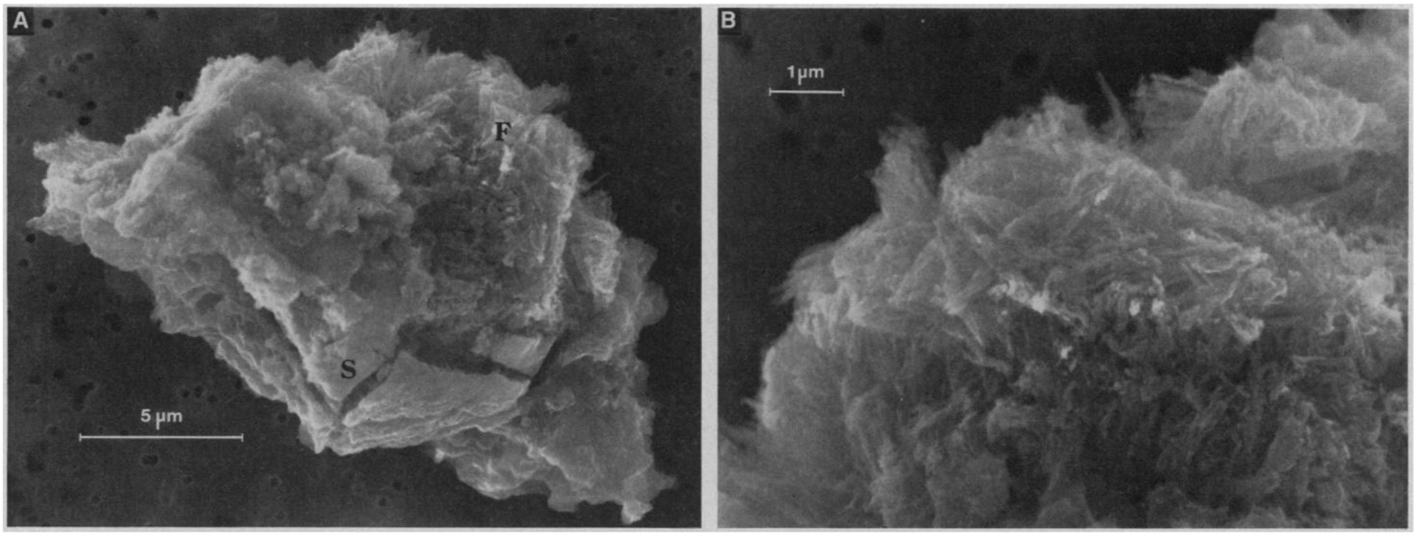

Fig. 1. Scanning electron micrographs of a fragment of RB12A44. (**A**) Low-magnification image showing both fibrous (F) and smooth (S) plate-like surface structures. The smooth regions are serpentine and the fibrous regions are finely intergrown serpentine (cronstedtite) and tochilinite [also known as PCP (*20–26*)]. (**B**) High-magnification image showing the distinctive fibrous morphology of the serpentine-tochilinite intergrowth.

RB12A44 exhibits both smooth, plate-like surfaces and fibrous regions (Fig. 1). The smooth surface structures are typical of layer-silicate IDPs (Fig. 1) (*7*), but the fibrous structures are unusual (Fig. 1B). We produced several ultramicrotomed thin sections (~50 nm thick) of the particle shown in Fig. 1 in order to examine its indigenous microstructures, mineralogy, and petrography (*13*). Solar flare tracks (with a density of $\sim 10^{11}$ cm^{-2}) were observed in several mineral grains (*16*), and the edges of some thin sections contained amorphous rims (10 to 20 nm thick), which are believed to result from direct exposure to the solar wind (*8, 17*).

Two principal mineral phases, serpentine and tochilinite (Figs. 2 and 3), were identified in thin section by lattice-fringe imaging, electron diffraction, and x-ray energy-dispersive spectrometry. Together, these minerals account for >95% of the volume of the IDP. Both Mg-rich and Fe-rich varieties of serpentine are present (Table 1). The serpentine exhibits characteristic basal lattice spacings of 7.0 to 7.3 Å, and the tochilinite exhibits both 5.4 and 10.8 Å spacings (Fig. 3). Most of the Fe-rich serpentine (cronstedtite) is intergrown with tochilinite on a unit-cell scale (Fig. 3). No crystals of pure (cronstedtite-free) tochilinite were identified. The most tochilinite-rich regions of the thin sections exhibit characteristic tubular microstructures (Figs. 2 and 3D). Pentlandite [$(\mathrm{FeNi})_9\mathrm{S}_8$], kamacite (FeNi alloy), troilite (FeS), magnetite ($\mathrm{Fe}_3\mathrm{O}_4$), and diopside [$(\mathrm{Ca,Mg})\mathrm{Si}_2\mathrm{O}_6$] are minor constituents in the matrices of RB12A44; single grains of schreibersite [Fe-Ni-(Cr)phosphide], (Fo_{84}) olivine, and an Mg-Fe-S-O phase (presumably sulfate) are also present. The schriebersite and olivine grains are almost 1 μm across, as are some of the pentlandite crystals, but the other mineral grains seldom exceed 200 nm in diameter.

The composition of the particle shown in Fig. 1 and the compositions of the major mineral phases identified in thin sections (Table 1) were determined by quantitative x-ray energy-dispersive spectrometry. We measured the bulk particle composition in the SEM using a correction procedure developed for analyses of small particles (Table 1, column 1) (*18*), and we analyzed thin sections in the AEM using a thin-film correction procedure (column 2) (*19*). Compositions were also determined for the tochilinite-cronstedtite intergrowths, cronstedtite, and Mg-rich serpentine (columns 3 to 6).

Tochilinite is an abundant (4 to 15% by weight) and ubiquitous constituent of the fine-grained matrices of type CM carbonaceous chondrites (*20–26*). It has not been found in any other meteorite (*20, 22, 25*). The presence of tochilinite thus implies that IDP RB12A44 is linked to CM chondrites. Its presence also suggests that RB12A44 was not strongly heated during atmospheric entry, because tochilinite is thermally unstable and converts rapidly to troilite at 245°C (*26*). Tochilinite is texturally distinct from any other minerals found in meteorites (Fig. 2). It is seldom found as crystals >100 nm, and as illustrated in Figs. 2 and 3, it is usually intergrown with cronstedtite on a unit-cell scale (*22, 23*). Although the crystal structure of tochilinite has yet to be verified by single crystal x-ray diffraction, it is believed to consist (ideally) of alternating sheets of Mg, Fe hydroxide, and Fe, Ni, (Cu) sulfide (*27*). The texture and composition of tochilinite provide key information for understanding the mechanism of aqueous alteration in the parent bodies of CM chondrites (*21–25*). Tomeoka and Buseck (*22*), for example, proposed that tochilinite and tochilinite-cronstedtite intergrowths (referred to as FESON and PCP, respectively) formed in the parent body regolith during a three-stage process of aqueous alteration. Their proposed sequence of mineralogical reactions is consistent with bulk compositional changes that have been observed to occur in the matrices of some CM chondrites that preserve differing degrees of aqueous alteration (*20, 25*).

The compositions and microtextures of tochilinite-cronstedtite intergrowths in RB12A44 are similar to those observed in the matrices of CM chondrites (compare Table 1, columns 3 to 8) (*22*), and most of the minor phases found in association with tochilinite in CM chondrites [for example, troilite, magnetite, pentlandite, and Fe-Ni-(Cr)-phosphide (*22*] are also found in RB12A44. The link to CMs is significant because there is evidence that this rare chondrite class [<2% of meteorite falls (*4*)] is abundant in space. The CM chondrites have the lowest albedo of all chondrites, and they show the best spectral and albedo match to the C asteroids that dominate the mid-region of the asteroid belt (*4, 28*). Fragments of CM material are the most common type of xenolith inclusions found inside other meteorites (*28*), and the ratio of siderophile elements to Ir of the meteoritic component of lunar soils suggests that CM-like material has provided a large amount of the material accreted to the moon over the past 3.7 billion years (*29*). The average oxygen isotopic composition of cosmic deep-sea spheres (melted 0.1- to 1.0-mm IDPs) is consistent with that of CM chondrites and distinct from that of CI and ordinary chondrites (*30*).

The apparent rarity of IDPs with CM-type mineralogy is also significant. Of almost 100 layer-silicate IDPs that have been

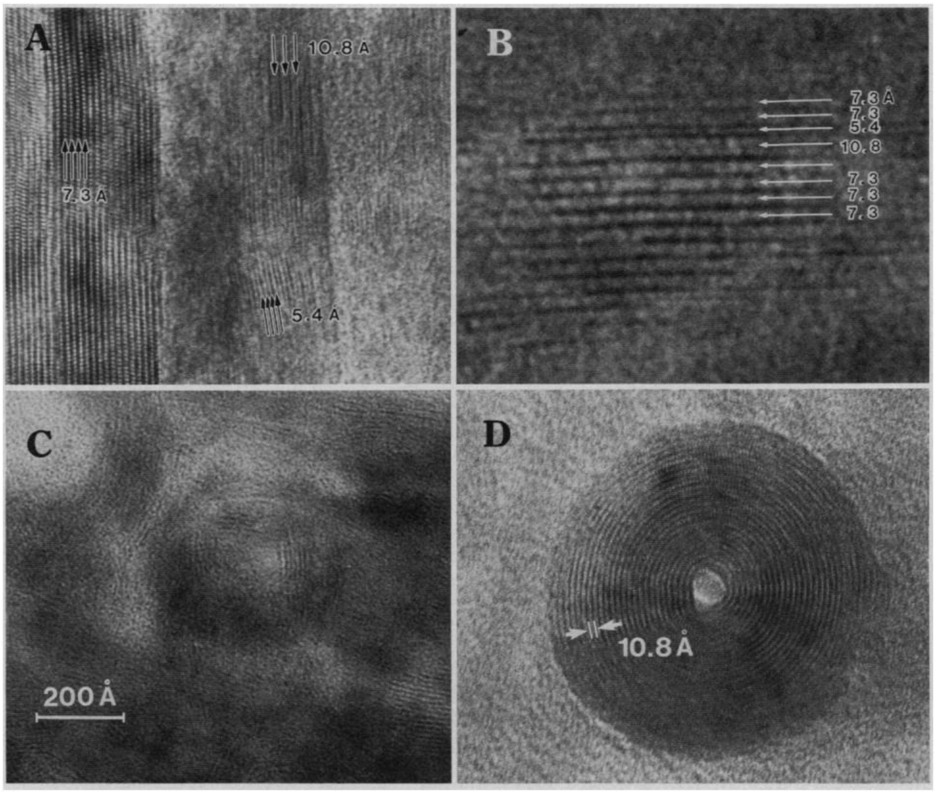

Fig. 3. Lattice-fringe images of cronstedtite and tochilinite in RB12A44. (**A**) Mixture of cronstedtite (7.3 Å spacing) and tochilinite (5.4 and 10.8 Å spacings). (**B**) Unit cell intergrowth of cronstedtite and tochilinite. (**C**) Psuedo-rectangular tochilinite "prototube" (*22*) nucleated in a cronstedtite plate. (**D**) Tochilinite tube.

studied by electron microscopy (*7, 12, 13, 31*), RB12A44 is the only one in which tochilinite and cronstedtite have been found. A specific search for these phases might reveal a higher abundance, but it is unlikely to exceed 10% of these IDPs. Therefore, if layer-silicate IDPs are a representative sampling of the asteroid belt, then CM chondrites cannot dominate the main belt, despite their similarity to the C reflectance class of asteroids (*28*). Both layer-silicate IDPs and C class asteroids could be samples of a broad spectrum of CM-like materials sharing common physical properties (for example, reflectance), but having significant mineralogical differences. For example, most layer silicate IDPs contain smectite rather than serpentine, and although the degree of aqueous alteration is variable from one IDP to another, it is often less than the matrices of CM chondrites (*13, 31*).

The identification of a CM-type IDP confirms predictions, based on calculations of particle orbital dynamics, that asteroidal material should be present among stratospheric IDPs (*6, 11*); most likely, materials from a variety of asteroidal parent bodies are present. However, only a subset of the IDPs have been studied. Most research has been focused on fine-grained IDPs because study of the variety of minerals they contain provides the best means for understanding their origins; coarser-grained IDPs have not yet been studied in detail. (Because of their coarse grain size, most meteorites could not be linked to a specific class of parent body on the basis of analysis of a 10-μm fragment.) In this study, we were able to make a strong link between RB12A44 and CM chondrites only because CMs are very fine grained and can be mineralogically distinct on a micrometer scale. If all layer-silicate IDPs are indeed of asteroidal origin, future sample studies combined with studies of dust dynamics should provide new information about geochemical conditions among the asteroids.

REFERENCES AND NOTES

1. S. A. Sandford, *Fundam. Cosmic Phys.* **12**, 1 (1987).
2. E. Anders, *Icarus* **24**, 363 (1975); G. W. Wetherill and C. R. Chapman, in *Meteorites and the Early Solar System*, J. F. Kerridge and M. S. Mathews, Eds. (Univ. of Arizona Press, Tucson, AZ, 1988), pp. 35–67.
3. E. Anders, in *Asteroids: An Exploration Assessment*, D. Morrison and W. C. Wells, Eds. (*NASA Publ. CP2053*, National Aeronautics and Space Administration, Houston, TX, 1978), pp. 316–335.
4. M. E. Lipschutz, M. J. Gaffey, P. Pellas, in *Asteroids II*, R. P. Binzel, T. Gehrels, M. S. Mathews, Eds. (Univ. of Arizona Press, Tucson, AZ, 1989), pp. 740–777.
5. Z. Sekanina, *Astron. J.* **90**, 827 (1985).
6. S. A. Sandford, *Icarus* **68**, 377 (1986); G. J. Flynn, *ibid.* **77**, 287 (1989); S. A. Sandford and J. P. Bradley, *ibid.* **82**, 146 (1989).
7. L. S. Schramm *et al.*, *Meteoritics* **24**, 99 (1989).
8. J. P. Bradley and D. E. Brownlee, *Science* **231**, 1542 (1986).
9. F. Verniani, *Space Sci. Rev.* **10**, 230 (1960).
10. J. S. Dohnanyi, in *Cosmic Dust*, J. A. M. McDonnell, Ed. (Wiley-Interscience, New York, 1978), pp. 527–605.
11. G. J. Flynn, *Proc. Lunar Planet. Sci. Conf.* **20**, 363 (1990).
12. K. Tomeoka and P. R. Buseck, *Earth Planet. Sci. Lett.* **69**, 243 (1984); I. D. R. MacKinnon and F. J. M. Rietmeijer, *Rev. Geophys.* **25**, 1527 (1987); K. L. Thomas, M. E. Zolensky, W. Klock, D. S. McKay, *Lunar Planet. Sci.* **XXI**, 1250 (1990); K. Tomeoka and P. R. Buseck, *Nature* **314**, 338 (1985).
13. J. P. Bradley, *Geochim. Cosmochim. Acta* **52**, 889 (1989).
14. R. E. Grimm and H. Y. McSween, Jr., *Icarus* **82**, 244 (1989).
15. Instruments used for this study were JEOL JSM-35C, 840, and 6400F SEMs, a 200-keV 2000FX AEM, and a 400-keV 4000FX AEM. All instruments were equipped with solid-state x-ray energy-dispersive spectrometers.
16. J. P. Bradley, D. E. Brownlee, P. Fraundorf, *Science* **226**, 1432 (1984).
17. K. Thiel, J. P. Bradley, R. Spohr, *Nucl. Tracks Rad. Meas.* **15**, 685 (1988); *ibid.*, in press.
18. J. T. Armstrong and P. R. Buseck, *Anal. Chem.* **47**, 2178 (1975).
19. G. Cliff and G. W. Lorimer, *J. Microsc.* **103**, 302 (1975); P. Sheridan, *J. Electron Microsc. Tech.* **11**, 41 (1989).
20. H. Y. McSween, Jr., *Geochim. Cosmochim. Acta* **51**, 2469 (1987).
21. K. Tomeoka and P. R. Buseck, *Nature* **306**, 354 (1983).
22. ———, *Geochim. Cosmochim. Acta* **49**, 2149 (1985).
23. K. Tomeoka, H. Y. McSween, Jr., P. R. Buseck, in *Proceedings of the Second National Institute for Polar Research Symposium on Antarctic Meteorites* (1989), p. 221.
24. M. E. Zolensky, *Meteoritics* **19**, 346 (1984).
25. E. Zolensky and H. Y. McSween, Jr., in *Meteorites and the Early Solar System*, J. Kerridge and M. S. Mathews, Eds. (Univ. of Arizona Press, Tucson, AZ, 1988), pp. 114–143.
26. L. Fuchs, E. Olsen, K. H. Jensen, *Smithson. Contrib. Earth Sci.* **10** (1973).
27. N. I. Organova, V. A. Drits, A. L. Dmitrik, *Am. Mineral.* **59**, 190 (1974); D. J. Barber, A. Bourdillon, L. A. Freeman, *Nature* **305**, 295 (1980); I. D. R. MacKinnon and M. E. Zolensky, *ibid.* **309**, 240 (1984).
28. J. Gradie, C. Chapman, E. Tedesco, in *Asteroids II*, R. P. Binzel, T. Gehrels, M. S. Mathews, Eds. (Univ. of Arizona Press, Tucson, AZ, 1989), pp. 316–335.
29. J. Wasson, W. V. Boynton, C. Chou, *Moon* **13**, 121 (1975).
30. R. N. Clayton, T. K. Mayeda, D. E. Brownlee, *Earth Planet. Sci. Lett.* **79**, 235 (1986).
31. M. S. Germani, J. P. Bradley, D. E. Brownlee, *ibid.* **101**, 162 (1990).
32. This research was supported by NASA grants NAS-9-17749 (J.P.B.), NSG 9052 (D.E.B.), and McCrone Associates. The Curatorial Facility at NASA Johnson Space Center provided IDP RB12A44. We thank L. Schramm, K. Tomeoka, A. Woodland, and M. Zolensky for constructive advice and J. Kerridge for detailed reviews.

27 September 1990; accepted 7 January 1991

A New Method for Carbon Isotopic Analysis of Protein

D. E. NELSON*

The reaction of ninhydrin with amino acids can be used in carbon isotopic studies of protein. The reaction can be applied to extract as carbon dioxide only peptide-bonded carbon in proteinaceous material, thus avoiding most, if not all, contaminants. Test radiocarbon dates on ancient bone indicate that the method provides reliable ages, and stable carbon isotopic data suggest that our understanding of isotopic dietary reconstruction needs detailed examination. The technique should also be useful in biochemical tracing experiments and in global carbon budget studies, and the underlying principle may be applicable to other isotopes and molecules.

AGE AND DIETARY INFORMATION obtained from carbon isotopic determinations on ancient bone is often contentious (*1, 2*) because of difficulties in isolating material uncontaminated by either diagenetic processes or laboratory procedures. Purity requirements are stringent, especially for radiocarbon dating of old samples, where admixtures of a few parts per thousand of contaminant carbon can cause serious errors. In most of the methods developed to solve this problem, an attempt is made to eliminate all possible contaminants from the sample (*3, 4*), whereas a few are designed for the extraction of only reliable material (*5–7*). In all cases, the material isolated is burned to yield the CO_2 used in isotopic analyses. Burning does not discriminate against contaminants and is known to be a source of carbon contamination (*8*). These methods do not provide internal measures of quality; one is never certain of sample purity and hence of the integrity of the result.

In this report I propose an alternative method; the use of a chemical reaction that selects specific carbon atoms from proteinaceous molecules. First tests indicate that this method is accurate, practical, and easily adapted for routine use in both radio- and

---

Center for Accelerator Mass Spectrometry, Lawrence Livermore National Laboratory, Livermore, CA 94550.

*Present address: Archaeology Department, Simon Fraser University, Burnaby, British Columbia, Canada V5A 1S6.